BIOCHEMISTRY
including biophysical chemistry & molecular biology
Article

Biochemistry **2010,** *49,* 8033–8042 8033
DOI: 10.1021/bi100451k

Distinct Extracytoplasmic Siderophore Binding Proteins Recognize Ferrioxamines and Ferricoelichelin in *Streptomyces coelicolor* A3(2)[†]

Prakash Patel, Lijiang Song, and Gregory L. Challis*

Department of Chemistry, University of Warwick, Coventry CV4 7AL, U.K.

Received March 25, 2010; Revised Manuscript Received August 12, 2010

ABSTRACT: Under iron limitation, the Gram-positive bacterium *Streptomyces coelicolor* A3(2) excretes three siderophores of the hydroxamate type: desferrioxamine B, desferrioxamine E, and coelichelin. These sequester iron from insoluble ferric hydroxides, and the resulting ferric complexes are believed to be transported into the cell via siderophore-binding proteins (SBPs) associated with ATP-binding cassette (ABC) transporters. Previous studies indicated that some of the genes in the desferrioxamine (*des*) and coelichelin (*cch*) biosynthetic clusters encode ABC transporter components required for efficient uptake of ferrioxamine E and ferricoelichelin, respectively, and a third ABC transporter gene cluster (*cdt*), not associated with siderophore biosynthesis genes, was implicated in the import of ferrioxamine B. In this study, the putative SBPs associated with these three gene clusters, DesE, CchF, and CdtB, were recombinantly overproduced in *Escherichia coli* and purified to homogeneity, and their binding affinity for cognate siderophores and noncognate siderophores was examined using fluorescence and circular dichroism spectroscopy. DesE was found to bind all of the ferric-*tris*-hydroxamates tested except ferricoelichelin, while CchF was found to bind only ferricoelichelin efficiently, providing further evidence that the *cch* cluster is a complete siderophore biosynthesis−export−uptake gene cluster. The picture was more complicated for CdtB, because it was found to be unstable in solution but was found to bind both ferrioxamine B and ferricoelichelin with high affinity. This was surprising because the *cch* cluster was previously reported to be necessary for efficient ferricoelichelin uptake. The remarkable specificity of the DesE and CchF proteins for different ferric-*tris*-hydroxamates raises intriguing questions about the molecular basis of their substrate specificity.

Siderophores are low molecular weight iron chelators that are produced by many microorganisms to scavenge ferric iron from hosts (in the case of pathogens) or the environment (in the case of saprophytes). They bind to ferric iron with high affinity, and the resulting ferric−siderophore complexes are shuttled back into cells via active transport mechanisms. The production of siderophores is a critical virulence factor for some pathogenic microorganisms that is required to establish infections in their hosts (*1*); for example, the stealth siderophore petrobactin has been shown to be important for growth of *Bacillus anthracis* in macrophages and virulence in mice (*2*).

In Gram-negative bacteria, extracellular ferrisiderophores are transported first into the periplasm via large β-barrel proteins called outer membrane receptors (OMRs). The substrate translocation is driven by the conformational change of the TonB−ExbB−ExbD complex at the cytoplasmic membrane, powered by the protonmotive force at the membrane (*1*). Once the ferrisiderophore is in the periplasm, the siderophore-binding protein (SBP)[1] component of an ATP-binding cassette (ABC) transporter binds to the complex. The ferrisiderophore is imported into the cytoplasm via interaction of the SBP−ferrisiderophore complex with the permease components of the ABC transporter (*3*).

In the case of Gram-positive bacteria (which lack a periplasm), the ferric−siderophore complexes are taken up via lipidated SBPs (also known as lipoprotein receptors) associated with the extracellular membrane surface by ABC transporters that are analogous to those of Gram-negative bacteria. The specificity of siderophore-binding proteins of the firmicute *Bacillus cereus* has been examined using both radiolabeled ferrisiderophore uptake experiments and the fluorescence quenching of purified recombinant SBPs by ferrisiderophores (*4*). Also, the structure of the ferric bacillibactin-binding SBP FeuA of *Bacillus subtilis* has been solved (*5*), showing that it is similar to SBPs of Gram-negative bacteria. The binding of ferrisiderophores to recombinant SBPs from *Staphylococcus aureus* and group B *Streptococci* has also been investigated (*6*, *7*). By contrast, there have been fewer studies on the uptake mechanisms of ferrisiderophores in Actinobacteria: only one protein has been identified as an importer of ferric-carboxymycobactin in *Mycobacterium tuberculosis* (*8*).

Streptomyces coelicolor A3(2) is a soil-dwelling, GC-rich, filamentous nonpathogenic actinomycete. Like many pathogenic microorganisms, *S. coelicolor* produces more than one siderophore. In particular, *S. coelicolor* produces three *tris*-hydroxamate siderophores (Figure 1), desferrioxamine B, desferrioxamine E,

[†]The EPSRC (MOAC Doctoral Centre, University of Warwick) funded this work.

*Corresponding author. Phone: (44) 2476 574 024. Fax: (44) 2476 524112. E-mail: g.l.challis@warwick.ac.uk.

[1]Abbreviations: FOB, ferrioxamine B; FOE, ferrioxamine E; CCLIN, ferricoelichelin; FCR, ferrichrome; ALB, ferrialbomycin; FeEnt, ferrienterobactin; ESI-MS, electrospray ionization mass spectrometry; SBP, siderophore-binding protein; ABC, ATP-binding cassette; RP-HPLC, reverse-phase high-performance liquid chromatography; SDS−PAGE, sodium dodecyl sulfate−polyacrylamide gel electrophoresis; NRPS, nonribosomal peptide synthetase; TAT, twin-arginine translocase; DmdR, divalent metal-dependent repressor; NIS, NRPS-independent siderophore synthetase; TEV, tobacco etch virus; NTA, nitrilotriacetic acid.

Published on Web 08/12/2010

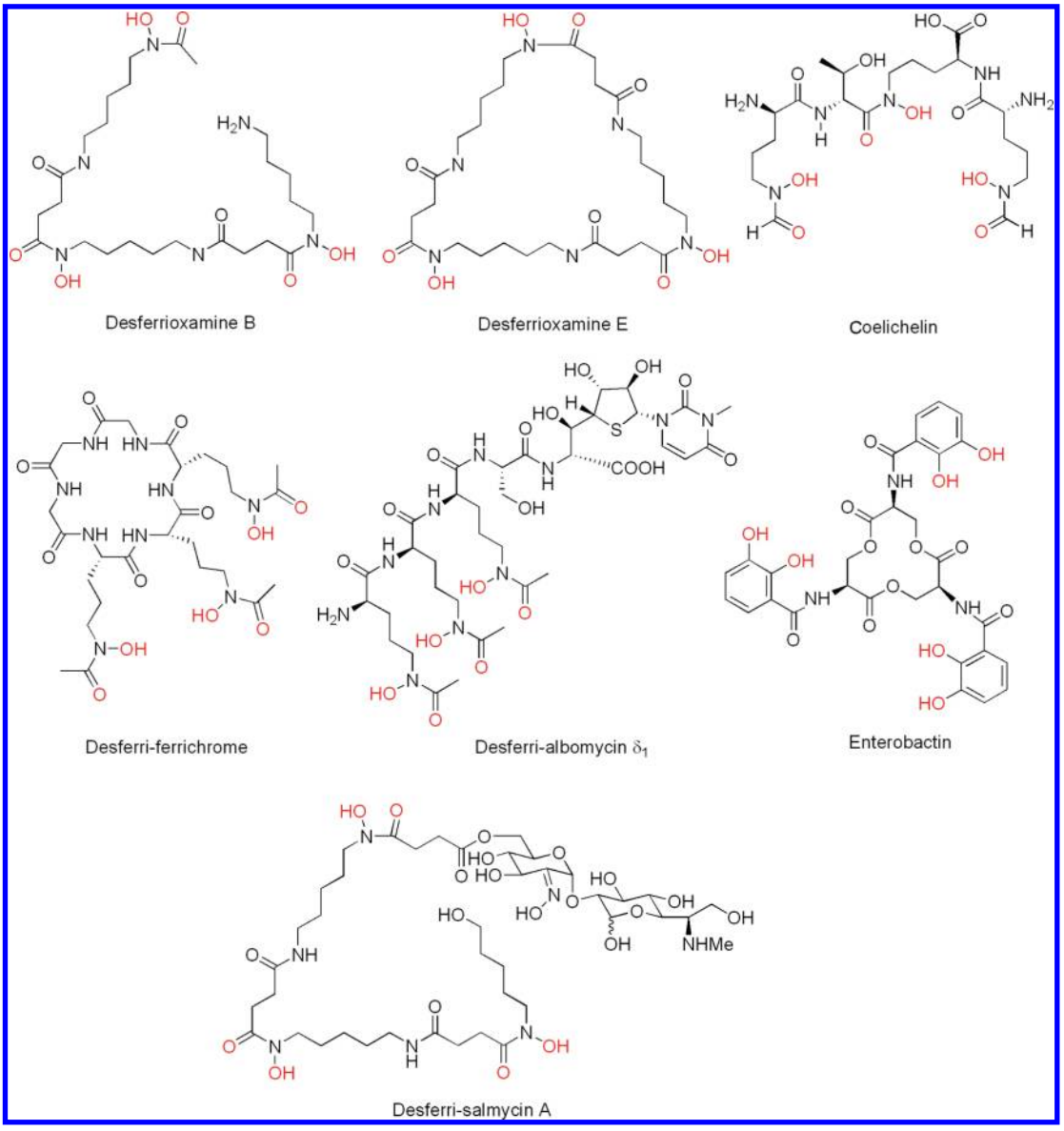

FIGURE 1: Molecular structures of siderophores used or discussed in this study. Desferrioxamine B, desferrioxamine E, and coelichelin are the cognate siderophores of *S. coelicolor*; the ferric complexes of these siderophores were used in this study (except for ferrisalmycin). The Fe(III) binding functional groups of the molecules are highlighted in red.

and coelichelin (*9*, *10*), under iron-limiting conditions. Many streptomycetes produce desferrioxamines, and many other organisms can utilize their ferric complexes as iron sources, while coelichelin production has been reported only in *S. coelicolor* A3(2) and *Streptomyces ambofaciens* ATCC28377 (*10*) to date.

The *des* cluster of genes (Figure 2) in *S. coelicolor* directs the production of desferrioxamines E and B(*11*). Roles for each of the *desABCD* genes in desferrioxamine biosynthesis have been proposed (*11*). DesD is a nonribosomal peptide synthetase independent siderophore (NIS) synthetase that catalyzes assembly of desferrioxamine E from three molecules of *N*-hydroxy-*N*-succinylcadaverine and desferrioxamine B from two molecules of *N*-hydroxy-*N*-succinylcadaverine and one molecule of *N*-acetyl-*N*-hydroxycadaverine (*12*, *13*). Immediately upstream of *desA* is a divalent metal-dependent regulator (DmdR) binding site. Ferrous−iron-dependent binding of DmdR proteins to this binding site controls the expression of *desABCD* (*14*).

While *desABCD* is involved in the biosynthesis of desferrioxamines, there are two genes upstream of *desA* (*desE* and *desF*), which also appear to be transcriptonally controlled by ferrous iron levels inside the cell, because there is a putative DmdR binding site upstream of *desE*. These genes were predicted to encode a lipidated extracellular SBP component of an ABC transporter (Table 1) and a siderophore-interacting protein (SIP), likely to be involved in the intracellular reduction of ferric−siderophores, respectively (*10*). DesE has been identified in the membrane-associated proteome (*15*) of *S. coelicolor*, contains an N-terminal prosite prokaryote lipidation site PS51257 (*16*), and is a twin-arginine translocase (Tat) substrate in *S. coelicolor* (*17*), suggesting this protein is associated with the extracellular membrane surface. The permease and ATPase components of the DesE-associated ABC transporter are not encoded by genes in the gene cluster, suggesting DesE would have to interact with other (as yet unidentified) ABC transporter permeases to transport ferrisiderophores.

Coelichelin production is directed by the *cch* cluster (Figure 2) of genes in *S. coelicolor* A3(2) and *S. ambofaciens* ATCC28377 (*9*, *10*). BLAST searches suggest that the *cch* cluster is also present in several other recently sequenced *Streptomyces* genomes (*vide infra*). The assembly of coelichelin is directed by the *cchH*

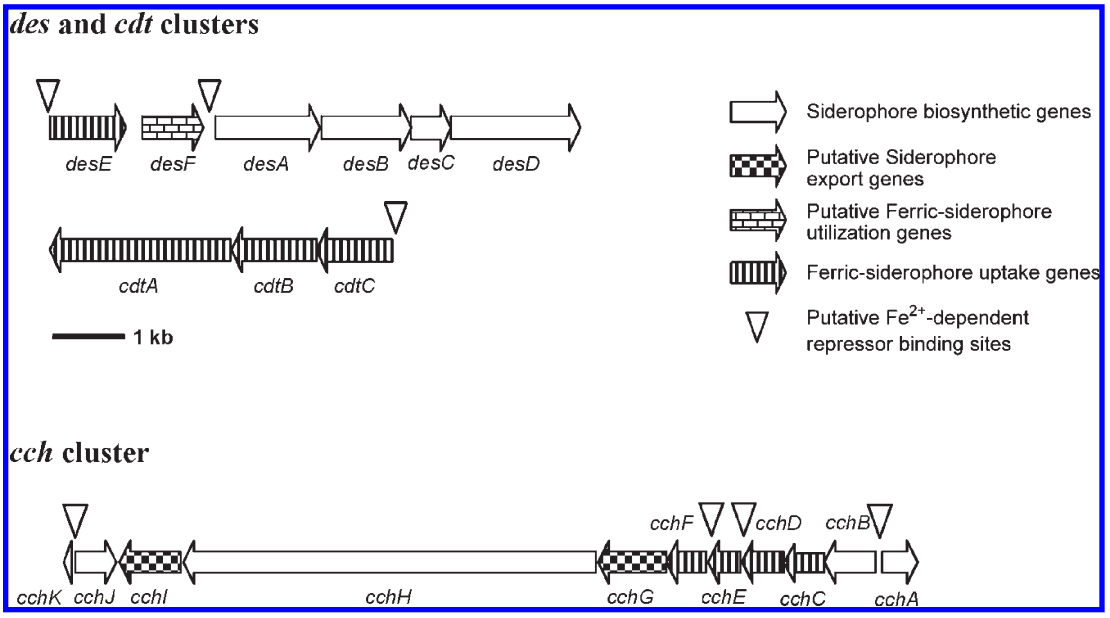

FIGURE 2: Organization of *S. coelicolor* gene clusters involved in siderophore biosynthesis and/or uptake.

Table 1: Calculated and Measured Characteristics of Putative Siderophore-Binding Proteins of *S. coelicolor*

protein	homologue (% identity)	native MW[a] (Da)	total AAs (signal sequence AAs)[b]	recombinant MW[c] (Da)	measured MW[d] (Da)
DesE	FhuD *B. subtilis* (24%)	36642	349 (30)	34590	34595
CchF	FhuD *B. subtilis* (26%)	37375	350 (31)	34915	34915
CdtB	FepB *E. coli* (24%)	34094	327 (21)	32770	32774

[a]Calculated molecular weights of the full-length native proteins. [b]Total number of amino acid residues in the native proteins; the number of N-terminal residues that were removed during cloning to facilitate purification of the proteins is shown in parentheses. [c]Calculated molecular weights of the purified recombinant proteins after cleavage of the His_6 tag. [d]Molecular weights of the purified recombinant proteins determined by ESI-TOF-MS analyses.

and *cchJ* genes, which encode an unusual trimodular nonribosomal peptide synthetase system that lacks a C-terminal thioesterase domain and an esterase, respectively (*9*). The export of desferricoelichelin is predicted to be directed by the *cchG* and *cchI* genes, while import of ferricoelichelin is proposed to be directed by the *cchCDEF* genes, which encode a complete ABC transporter (*10*). The *cchF* gene encodes an SBP, *cchC* and *cchD* encode permeases, and *cchE* encodes an ATPase (*10*).

To investigate the role of ABC transporter components encoded within the *des* and *cch* gene clusters of *S. coelicolor* in siderophore uptake, Barona-Gomez et al. constructed siderophore nonproducing mutants of *S. coelicolor* in which the *des* and *cch* gene clusters were deleted (*10*). Siderophore nonproducing mutants that had only the *desD* and *cchH* genes deleted were also made (*10*). The *cch* and *des* cluster deletion mutants lack the DesE and CchF siderophore-binding proteins, while the *desD* and *cchH* mutants still contain these receptors. The various mutants were grown on iron-deficient colloidal silica plates (which lack xenosiderophores), and the growth halos around filter paper disks supplemented with different siderophores were observed. The *des* cluster mutant was unable to grow well when supplemented with ferrioxamine E and the fungal siderophore ferrichrome, while the *cch* cluster mutant could not grow when supplemented with ferricoelichelin. Surprisingly, all of the mutants, including ones where both *des* and *cch* clusters were deleted, were able to grow well with ferrioxamine B supplementation. These results suggest the SBP DesE is necessary for efficient uptake of ferrioxamine E and ferrichrome in *S. coelicolor*, while the SBP CchF is necessary for ferricoelichelin uptake, and another transport system, independent of the *des* and *cch* clusters, is able to uptake ferrioxamine B. The *cdtABC* gene cluster (SCO7398-7400) (Figure 2) was hypothesized to encode the ferrioxamine B ABC transporter (*10*). The *cdtA* gene encodes two permease domains of an ABC transporter, while the *cdtB* gene encodes a SBP, and the *cdtC* gene encodes an ATPase. A putative DmdR binding site was identified upstream of the ATPase gene *cdtC*.

In an independent study to determine whether the *cdtABC* gene cluster had a role in siderophore uptake (*18*), the gene cluster was replaced by an apramycin resistance cassette, and the resulting mutant was grown in the presence of ferrisalmycin (*19*), a siderophore−antibiotic conjugate analogous to ferrioxamine B (Figure 1). It was found that the mutant was not sensitive to ferrisalmycin, while wild-type *S. coelicolor* was, and that this was not due to the presence of the apramycin-resistance gene used to replace *cdtABC*. Supplementation with ferrioxamine B reduced the sensitivity of the wild-type *S. coelicolor* to ferrisalmycin on solid media, although uptake experiments with radioactive ^{55}Fe-ferrioxamine B suggested there was no difference in uptake of this siderophore between the wild type and the mutant, suggesting the presence of a second ferrioxamine B transport system. These results show CdtB is required for ferrisalmycin uptake, a process that is competitively inhibited by ferrioxamine B, suggesting that CdtB may be a ferrioxamine B binding protein.

Several other putative SBPs have been identified in *S. coelicolor*, many of them adjacent to ABC transporter genes, in particular SCO2272, SCO0996, and SCO7218 (*18*), but so far have not been shown to have a role in siderophore-mediated iron acquisition. DesE, CchF, and CdtB are the only SBPs that have been identified in the membrane-associated proteome of *S. coelicolor* (*15*).

In this study, DesE, CchF, and CdtB were overproduced in *Escherichia coli* and purified by immobilized metal-affinity chromatography. The quenching of intrinsic fluorescence and CD spectroscopy were used to examine the binding of various ferri- and desferrisiderophores to the proteins, including the three cognate siderophores of *S. coelicolor*.

EXPERIMENTAL PROCEDURES

Cloning of SBP-Encoding Gene Fragments. Fragments of *desE*, *cchF*, and *cdtB* truncated to the cysteine codon corresponding to the lipid attachment site (closest to the 5′ end) were amplified by PCR from the cosmids SCC105, SCF34, and *S. coelicolor* genomic DNA, respectively. PCR amplification was performed by a single round of denaturation (94 °C for 2 min) and discrete cycles of denaturation (94 °C for 45 s), annealing (55 °C for 45 s), and extension (72 °C for 90 s), followed by a single extension (72 °C for 15 min) using Expand high fidelity polymerase (Roche). The primers desE_forward CACC**ATG**GGCGACGGCGACGGCAAG and desE_reverse TCAGCCGACCTTCTTGGCGT were used to amplify the *desE* fragment, cchF_forward CACC**ATG**GGATCCGACTCGGACGA and cchF_reverse CTACCCGGCCGACTTGACGA were used to amplify the *cchF* fragment, and cdtB_forward CACC**ATG**GGCACCACCGAACCCG and cdtB_reverse CTACTTCGTCAGCGCGCCGACGAC were used to amplify the *cdtB* fragment. The 5′-CACC extension (required for directional TOPO cloning) is underlined in the forward primers, and the methionine codon which was introduced to replace the N-terminal cysteine codon is highlighted in bold. The amplimers were purified by using a QIAGEN gel extraction kit (Qiagen Inc.) and cloned into the pET151/D-TOPO vector using the Champion pET Directional TOPO expression kit (Invitrogen). Clones containing the expected insert sizes, confirmed by PCR using the original primers and *Taq* polymerase (Invitrogen), were sequenced. Purified plasmid DNA from clones with the correct insert sequence and orientation were used to transform chemically competent *E. coli* BL21star (DE3) cells (Invitrogen). The plasmids used for overproduction of N-terminal truncated DesE, N-terminal truncated CchF, and N-terminal truncated CdtB are denoted pPP001, pPP002, and pPP003, respectively.

Overproduction of Recombinant N-Terminal Truncated SBPs. An overnight culture of *E. coli* BL21star (DE3) containing the requisite expression plasmid was inoculated (0.3% v/v) into 600 mL of LB medium containing ampicillin (50 μg mL^{-1}), and the resulting culture was grown at 37 °C with shaking at 180 rpm for 3 h. Protein overproduction was induced by addition of IPTG (0.5 mM) when the culture reached an $OD_{600} \approx 0.6-0.8$. After induction the cultures were incubated at 15 °C for 12 h. Cells were harvested by centrifugation at 8000*g* for 20 min. In the case of CdtB the cell pellets were frozen overnight at −20 °C prior to protein purification. For DesE and CchF, the purification was carried out immediately after harvesting of the cells.

Purification of His_6-Tagged Recombinant SBPs. The cell pellets were resuspended in washing buffer (10 mM Tris-HCl, pH 8.0, 100 mM NaCl, 20 mM imidazole, and 10% glycerol), and 10 μM PMSF was added to inhibit proteases. The cells were lysed using a French pressure cell press (Thermo Scientific) at 4 °C using the 40K standard cell (Thermo Scientific) at a pressure of 20000 psi. The lysate was centrifuged (15000*g*, 20 min) to remove cell debris. Recombinant proteins were purified by nickel-immobilized affinity chromatography (Ni-IMAC) on a 1 mL HisTrap Ni-NTA Sepharose column (GE Healthcare) using an AKTA purifier (Amersham Biosciences, GE Healthcare) with the detector wavelength set at 280 nm. The column was washed with 20 mL of washing buffer to remove nonspecifically interacting proteins, and His_6-tagged proteins were eluted with elution buffer (10 mM Tris-HCl, pH 8.0, 100 mM NaCl, 300 mM imidazole, and 10% glycerol). Proteins were concentrated using a 30000 molecular weight cutoff 15 mL Amicon ultracentrifugal filter (Millipore) and stored at −80 °C in gel filtration buffer (10 mM Tris-HCl, pH 8.0, 100 mM NaCl, and 10% glycerol). The purity of the protein was assessed by electrophoresis on an 8% SDS−PAGE gel stained with Coomassie Brilliant Blue R250. Protein concentrations were measured using the Bradford assay (*20*).

Cleavage of the His_6 Tag from Purified SBPs. The *E. coli* BL21(DE3)-RIL strain transformed with pRK793 overproducing an autoinactivation resistant S219V mutant recombinant TEV protease catalytic domain with an N-terminal His tag was purified according to a standard protocol (*21*). Purified His-tagged TEV protease was added to His_6-tagged recombinant protein (approximate molar ratio 1:50), and the resulting solution was incubated for 12−15 h at 4 °C. Digestion product (0.5−1 mL) was passed through a 1 mL HisTrap column with washing buffer. The flow-through was collected and concentrated by centrifugal filter. The proteins were analyzed by SDS−PAGE to assess purity.

Gel Filtration Analysis of Recombinant SBPs. A solution of protein (500 μL) was loaded onto a size exclusion column (HiLoad 75 Superdex 12 prep grade resin, column volume 110 mL; Amersham Biosciences) equilibrated with gel filtration buffer at 0.8 mL/min, connected to an AKTA purifier (Amersham Biosciences, GE Healthcare). The column was eluted with isocratic gel filtration buffer. Five milliliter fractions were collected in the case of preparative gel filtration. Absorbance at 280 nm was monitored. The column was calibrated with the kit for molecular weights 12000−200000 Da (Sigma), consisting of cytochrome *c* (12400 Da), carbonic anhydrase (29000 Da), bovine serum albumin (66000 Da), alcohol dehydrogenase (150000 Da), β-amylase (200000 Da), and Blue dextran (2000000 Da), which eluted at volumes of 89.2, 71.5, 59.6, 56.1, 52.9, and 40.1 mL, respectively.

Mass Spectrometric Characterization of Purified Recombinant Proteins. Proteins were dialyzed five times in 10 mM ammonium acetate (pH 7.0) using a 10000 molecular weight cut off spin filter (Vivaspin, Millipore Inc.) to give a final concentration of 25 μM. The solution was acidified by adding 10 μL of 50% aqueous acetonitrile acidified with 0.1% trifluoroacetic acid. A total volume of 60 μL of protein solution was injected continuously into a Bruker micrOTOF electrospray ionization mass spectrometer (Bruker Daltonics, Coventry, U.K.) using the following settings: positive ion mode, scan range m/z 800−5000, capillary exit voltage 250.0 V, skimmer voltage 90.1 V, hexapole 24.8 V, hexapole RF voltage 750.0 V, corrector fill 48 V, pulsar pull 369 V, pulsar push 369 V, reflector 1300 V, flight tube 9000 V, and detector TOF 2140 V. The spectra were analyzed and deconvoluted to identify multiply charged species using Bruker Daltonics DataAnalysis 3.3 software (Bruker Daltonics, Coventry, U.K.). The identities of the proteins were confirmed by peptide mass fingerprinting performed by the Biological Mass Spectrometry and Proteomics Facility in the Department of Biological Sciences, University of Warwick.

Circular Dichroism Spectroscopic Analysis of Purified SBPs. DesE and CchF were dissolved in 10 mM sodium

phosphate buffer (pH 7.0) to a final concentration of 80 μg/mL 3 h prior to analysis. Ferrisiderophores were added to a final concentration of 5 μM and incubated for 5 min at 21 °C prior to analysis. The instrument used was a Jasco J-715 spectropolarimeter with excitation slit length of 1 nm. A 1 mm path length quartz cuvette was used to hold the sample. The spectra were recorded from 190 to 250 nm, and eight scans were accumulated. The spectrum of the solvent was subtracted upon processing.

Spectra of freshly prepared CdtB in the presence/absence of ferrioxamine B and in the absence of ferrioxamine B after 2 h of standing at 21 °C were recorded on a Jasco-815 spectrometer. CdtB was dissolved in 10 mM sodium phosphate buffer (pH 7.0) to give a final concentration of 3 μM. Ferrioxamine B was added to a final concentration of 3 μM. A 1 mm path length cuvette was used, and spectra were the average of two scans. The melting temperature of CdtB in the presence/absence of ferrioxamine B was determined as described previously, (*5*) except 10 mM sodium phosphate buffer was used, the protein and siderophore concentrations were both 3 μM, and the change in circular dichroism at 195 nm was monitored.

Fluorescence Spectroscopy. Fluorescence quenching of recombinant SBPs upon siderophore binding was monitored on a Perkin-Elmer LS 50B luminescence spectrometer with an excitation wavelength of 280 nm. Proteins were dissolved in 100 mM phosphate-buffered saline (pH 7.0) to a final concentration of 0.78 mg/mL. In the case of CchF it was incubated at 37 °C for 45 min prior to dissolving in phosphate-buffered saline. No cutoff filters were used in the course of the experiments. The fluorescence spectrum was recorded from 310 to 380 nm, with a scan speed of 50 nm/min. The excitation and emission slit lengths were 5.0 and 8.0 nm, respectively, except in the case of CchF where they were 5.0 and 10.0 nm, respectively. The measurements were taken using a 3 mm path length quartz cuvette (Starna Scientific) with the total volume ranging from 90 to 100 μL. Siderophore solutions were titrated into the protein solutions, mixed by agitation with a micropipet tip, and incubated in the cuvette for 4 min at 21 ± 1 °C before recording the spectra. The titrations were repeated at least three times.

Processing of Fluorescence Data. The fluorescence at 335 nm was used to monitor the relative proportion of binding of different concentrations of ligand to DesE and CdtB. In the case of CchF, the fluorescence was monitored at 325 nm. With tight-binding siderophores (small K_D), the fluorescence of the bound protein F_{min} was estimated by addition of a large concentration of siderophore into the protein solution. The data were linearly transformed in Microsoft Excel into proportion bound using eq 1.

$$\text{proportion of protein bound to ligand} = \frac{F_0 - F}{F_0 - F_{min}} \quad (1)$$

F_0 is the fluorescence of unbound protein, F is the fluorescence of the protein−ligand solution, and F_{min} is the fluorescence of the ligand-saturated protein. The transformed data were copied into Origin 6.0 Professional (*22*), and the nonlinear curve fitting function was used to fit the data to find the dissociation constant K_D using eq 2.

$$\frac{F_0 - F}{F_0 - F_{min}} = \frac{K_D + [P_T] + [L_T] - \sqrt{((K_D + [P_T] + [L_T])^2 - 4[P_T][L_T])}}{2[P_T]} \quad (2)$$

$[L_T]$ is the total ligand concentration, and $[P_T]$ is the protein concentration.

For relatively weak interactions between siderophores and SBPs, F_{min} had to be estimated, as in the case of ferrisiderophore binding to CchF and CdtB. A provisional value of F_{min} was used derived from CchF bound to high concentrations of ferricoelichelin and CdtB bound to high concentrations of ferrioxamine B. The data were linearly transformed into "relative fluorescence decrease compared to F_{min}(siderophore)" by the relation $Q = (F_0 - F)/(F_0 - F_{min}(\text{siderophore}))$ in Microsoft Excel. The transformed data were fit to the coupled eqs 3 and 4 of Ahnström et al. (*23*) using the nonlinear curve fitting function in Origin 6.0 Professional (*22*) to find K_D and Q simultaneously.

$$\frac{F_0 - F}{F_0 - F_{min}} = Q\left(\frac{[L]}{[L] + K_D}\right) \quad (3)$$

$$[L] = \frac{[L_T] - K_D - [P_T]}{2} + \sqrt{\left(\frac{[L_T] - K_D - [P_T]}{2}\right)^2 + K_D[L_T]} \quad (4)$$

The concentration of free ligand, [L], links eqs 3 and 4.

Preparation of Ferri- and Desferrisiderophores for Binding Experiments. The purification of gallium−coelichelin was carried out using a modification from the previously described method (*9*). The processed culture supernatant of iron-deficient cultures of *S. coelicolor* M145 containing ferricoelichelin was separated by reverse-phase HPLC (Agilent Zorbax C-18 column, 21.2 × 10.0 mm, 5 μm particle size, temperature 20 °C) using the mobile phases H_2O (0.1% trifluoroacetic acid):acetonitrile (0.1% TFA) with the following elution profile: 0 min 1:0; 15 min 9:1; 20 min 0:1; 30 min 0:1; 35 min 1:0; 45 min 1:0. A yellow eluate was collected at 7.0 min, which was confirmed to be ferricoelichelin by the presence of the *m*/*z* 619 ion in the ESI-TOF mass spectrum. The preparation and purification of desferricoelichelin from the combined ferricoelichelin-containing fractions and the subsequent preparation of gallium−coelichelin were performed as described previously (*9*). Gallium−coelichelin was purified by RP-HPLC using an Agilent Zorbax C-18 column, and its identity was confirmed by ESI-TOF-MS and ^{1}H NMR spectroscopic analysis. Ferricoelichelin was prepared by addition of an excess of $FeCl_3$ to gallium−coelichelin, followed by reaction for 15 h at 4 °C. The identity of ferricoelichelin was confirmed by mass spectrometry, UV−visible spectroscopy (large absorption at 420−435 nm typical of ferri-*tris*-hydroxamates), and HPLC-MS comparison with culture supernatants of *S. coelicolor* M145. The concentration of ferricoelichelin was determined by inductively coupled plasma optical emission spectroscopy (ICP-OES) at emission wavelengths of 238.204, 239.562, and 259.939 nm (specific for the detection of iron), compared to dilutions of an iron for AAS standard solution 1001 ± 3 mg/L (Fluka).

Desferrioxamine B was obtained from Sigma-Aldrich. Ferrioxamine B was produced by addition of an excess of $FeCl_3$ to desferrioxamine B and purification by RP-HPLC using the method described above for separating the processed culture supernatant of iron-deficient cultures of *S. coelicolor* M145. All other ferri- and desferrisiderophores were purchased from EMC Microcollections GmbH Tübingen. The concentrations of ferrisiderophore solutions were determined by UV−vis spectroscopy using published extinction coefficients (*24*) and/or ICP-OES.

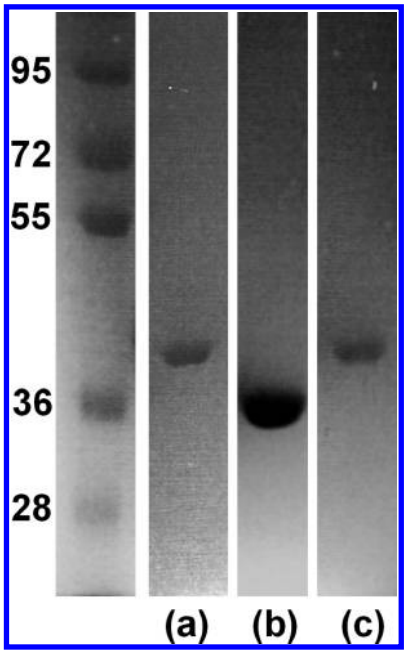

FIGURE 3: SDS−PAGE analysis of purified recombinant SBPs of *S. coelicolor*: (a) DesE; (b) CchF; (c) CdtB against molecular weight markers (first lane) whose sizes are given in kDa.

RESULTS

Overproduction and Purification of Recombinant SBPs. DesE, CchF, and CdtB lacking the N-terminal signal sequence and with the N-terminal cysteine residue that is the site of lipidation after signal peptide cleavage mutated to methionine were overproduced in *E. coli* as N-terminal His_6 fusions with a downstream TEV protease cleavage site. After purification by Ni-NTA affinity chromatography, the His_6 tags were removed using TEV protease and purified to homogeneity by a second pass through a Ni-NTA column (Figure 3). The identities of the proteins were confirmed by peptide mass fingerprinting (data not shown) and ESI-TOF-MS analysis (Table 1). To analyze the oligomerization state of the SBPs in solution, gel filtration was used. DesE and CdtB were found to be monomeric, whereas CchF was predominantly monomeric but contained a small quantity of an oligomer (probably a trimer; see Supporting Information). Gel filtration analysis of CchF after incubation at 37 °C for 45 min showed that it was converted entirely to the monomeric form. Since the interpretation of the results of experiments carried out on a mixture of different oligomeric forms was likely to be complicated, we carried out all experiments on entirely monomeric CchF.

Siderophore Binding to DesE. The fluorescence of DesE was quenched significantly by ferrioxamines B and E, ferrichrome, and ferrialbomycin (Figure 4), indicating strong interactions of these ferrisiderophores with DesE. On the other hand, no significant fluorescence quenching was observed upon addition of ferricoelichelin, indicating that this cognate ferrisiderophore of *S. coelicolor* does not bind to DesE. No significant quenching was observed on addition of desferrioxamines E and B, desferrichrome, ferrienterobactin, or desferrienterobactin. F_{min} could be estimated by addition of large concentrations of ferrisiderophores; hence eqs 1 and 2 (Experimental Procedures) were used to transform the raw fluorescence data. The dissociation constants calculated for ferrioxamine B, ferrioxamine E, and ferrichrome from the data were in the nanomolar range (Table 2).

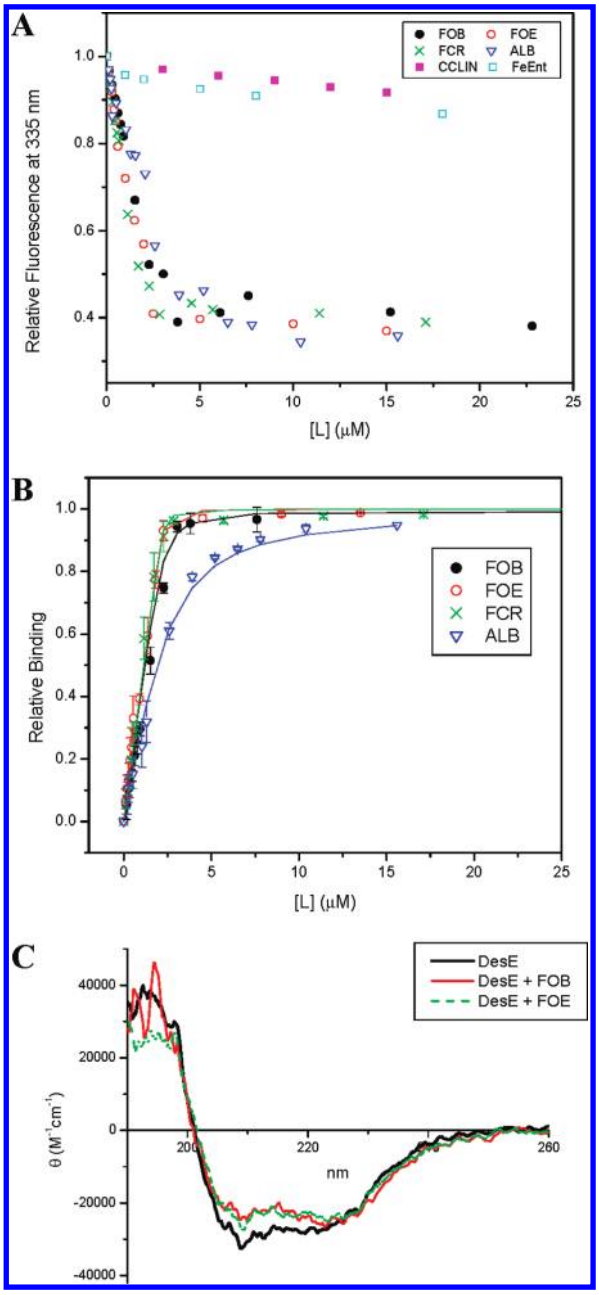

FIGURE 4: Normalized fluorescence quenching, relative binding curves, and CD spectra for binding of ferrisiderophores to purified recombinant DesE. (A) Normalized fluorescence of DesE in the presence of varying concentrations of ferrisiderophores. (B) Relative binding of ferrisiderophores to DesE. Curve fitting gave rise to the K_D values shown in Table 2. (C) CD spectra of DesE with and without addition of ferrioxamines E and B.

Siderophore Binding to CchF. The fluorescence of CchF was significantly quenched by low concentrations of ferricoelichelin (Figure 5), indicating a strong interaction. As F_{min} could be estimated by addition of large concentrations of ferrisiderophore to the protein solution, eqs 1 and 2 (Experimental Procedures) were used to calculate a dissociation constant. Relatively high concentrations of ferrioxamine B and ferrialbomycin were needed to quench the fluorescence of CchF significantly. F_{min} could not be calculated by addition of large concentrations of these ferrisiderophores; hence the F_{min} value estimated with ferricoelichelin was used in eq 1 to transform the data (Experimental Procedures), and eq 3 was used to find K_D (Table 2). High concentrations of ferrioxamine E and ferrichrome were unable to

Table 2: Calculated Dissociation Constants K_D (in μM) of *S. coelicolor* SBPs from Ferric-*tris*-hydroxamate Siderophores Determined by Fluorescence Quenching Experiments[a]

ligand	DesE	CchF	CdtB (100%)	CdtB (75%)
ferrioxamine B	0.090 ± 0.040	37.1 ± 6.4[b]	0.080 ± 0.024	0.100 ± 0.056
ferrioxamine E	0.011 ± 0.009	nd[c]	8.7 ± 1.9[b]	8.9 ± 1.8[b]
ferricoelichelin	nd[c]	0.33 ± 0.02	0.039 ± 0.021	0.172 ± 0.023
ferrichrome	0.013 ± 0.009	nd[c]	77 ± 3[b]	77 ± 3[b]
ferrialbomycin	0.750 ± 0.066	20.4 ± 3.6[b]	12.3 ± 0.4[b]	12.6 ± 0.4[b]

[a]For CdtB, two different constants were calculated on assumption 100% and 75% of the protein were able to participate in ferrisiderophore binding, respectively. [b]K_D was determined by simultaneously estimating F_{min} using the equations of Ahnström et al. [c]nd: not determined due to insufficient protein fluorescence quenching by ferrisiderophore.

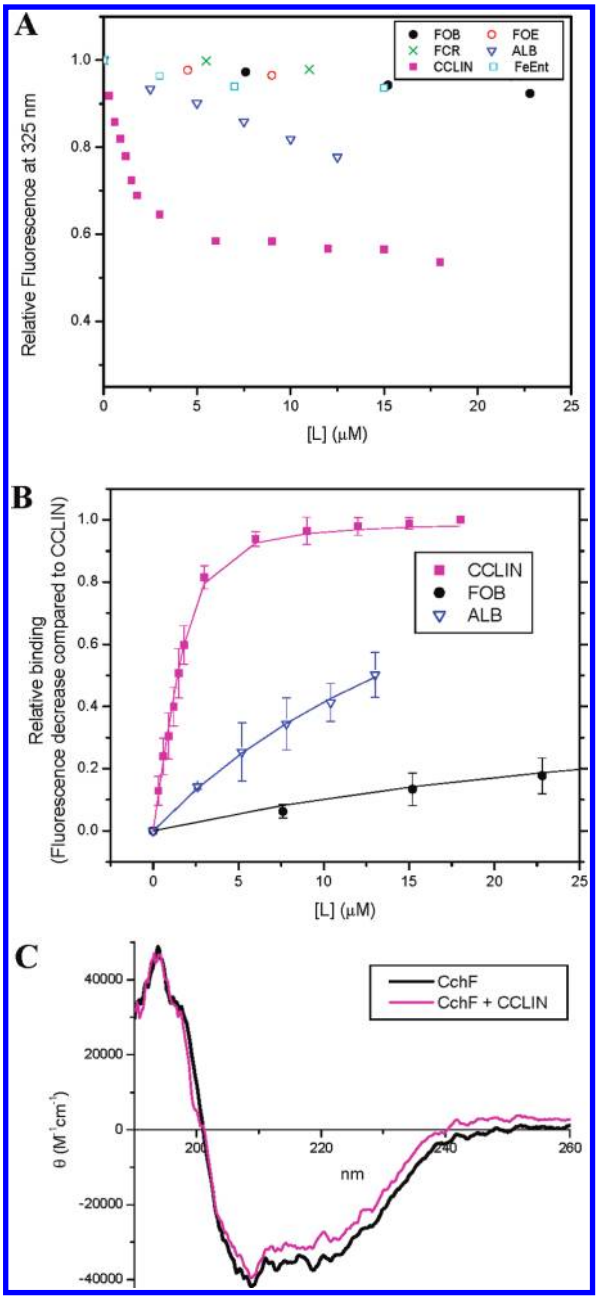

FIGURE 5: Normalized fluorescence quenching, relative binding curves, and CD spectra for binding of ferrisiderophores to purified recombinant CchF. (A) Normalized fluorescence of CchF in the presence of varying concentrations of ferrisiderophores. (B) Relative binding of ferricoelichelin to CchF and relative fluorescence decrease of CchF upon addition of ferrioxamine B and ferrialbomycin compared to ferricoelichelin. Curve fitting gave rise to the K_D values shown in Table 2. (C) CD spectra of CchF with and without addition of ferricoelichelin.

quench CchF fluorescence sufficiently to allow dissociation constants to be determined. This was also the case with desferrioxamines B and E, desferriferrichrome, enterobactin, and ferrienterobactin.

CdtB Is Unstable in Solution. Unlike DesE and CchF, the fluorescence of CdtB solutions decreased almost linearly over time upon standing (Figure 6), with the wavelength of the emission maximum increasing from 335 to 340 nm. The most plausible explanation for this is that the protein unfolds readily at room temperature. The tryptophan residues are exposed to the solvent as the protein unfolds, resulting in quenching of their fluorescence by water and a red shift in the emission toward the emission maximum of free L-tryptophan in water (348 nm). Investigation of how the CD spectrum of CdtB changed with time confirmed this hypothesis (see below).

Siderophore Binding to CdtB. Despite the instability of CdtB, the quenching of fluorescence upon addition of ferrioxamine B, ferricoelichelin, and ferrialbomycin was significant even after 3 h at room temperature. High concentrations of ferrioxamine E and ferrichrome caused some quenching of CdtB fluorescence. The experiments were carried out within 3 h (the protein was assumed to remain largely folded over this period). F_{min} could be estimated in the case of ferricoelichelin and ferrioxamine B by addition of high concentrations of siderophore, but in the case of ferrioxamine E, ferrichrome, and ferrialbomycin there was insufficient quenching to calculate F_{min}; hence the F_{min} value estimated with ferrioxamine B was used with eq 1 to transform the data (Experimental Procedures), and eq 3 was used to find K_D. Two values of K_D were calculated by assuming that 100% and 75% of the protein were able to participate in ligand binding (Table 2). The assumption that a smaller proportion than 75% of CdtB was able to participate in ligand binding was unable to provide adequate curve fits to the fluorescence data. Consistent with this, estimation of the equivalence point for titrations of CdtB with ferrioxamine B indicated that only about 85% of the initial ferrioxamine B binding sites are present after the protein has been left to stand at room temperature for 2 h. No such decrease in ferrisiderophore binding sites was observed for DesE, using a similar analysis, when it was left to stand at room temperature. Desferrioxamine B, desferrioxamine E, desferriferrichrome, enterobactin, and ferrienterobactin did not cause significant quenching of CdtB fluorescence.

Circular Dichroism Spectroscopy of SBPs. The observed instability of CdtB prompted us to examine the folding state of SBPs using CD spectroscopy (*25*). The CD spectra of DesE and CchF (Figures 5 and 6) are indicative of fully folded proteins with prominent α-helical content (negative signals at 206 and 220 nm). CD spectroscopic analysis of freshly prepared CdtB indicated that it is also essentially fully folded with high α-helix content

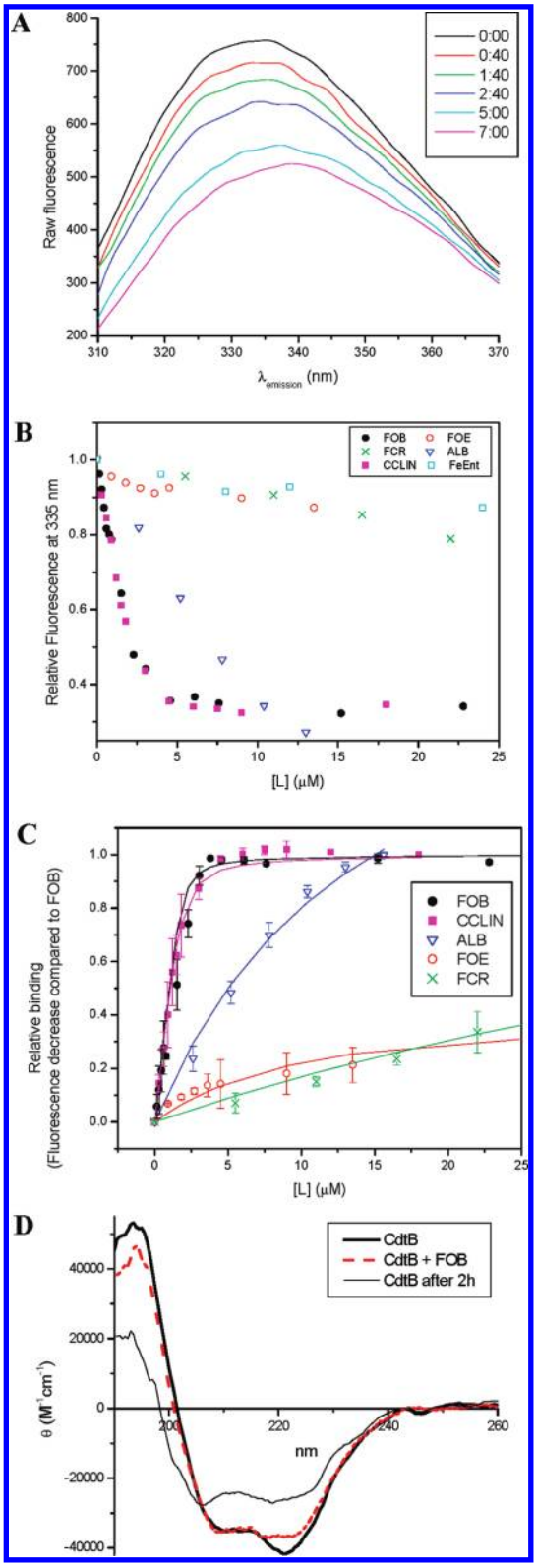

FIGURE 6: Change in fluorescence over time, normalized fluorescence quenching, relative binding curves, and CD spectra on addition of ferrisiderophores for purified recombinant CdtB. (A) Fluorescence spectra of CdtB from 310 to 370 nm with elapsed time in hours: minutes after preparation of solution. (B) Normalized fluorescence of CdtB on addition of ferrisiderophores. (C) Relative binding of ferrioxamine B and ferricoelichelin to CdtB and relative fluorescence decrease of CdtB caused by addition of ferrioxamine E, ferrichrome. and ferrialbomycin compared to ferrioxamine B. Curve fitting yielded the K_D values shown in Table 2. (D) CD spectra of freshly prepared CdtB with and without addition of ferrioxamine B and CD spectrum of CdtB after 2 h at 21 °C.

(Figure 6). However, upon standing at room temperature the signals at 195, 206, and 220 nm in the CD spectrum of CdtB decreased in intensity, confirming that this protein is unstable and unfolds. Addition of ferrisiderophores that bind tightly to DesE, CchF, and CdtB did not cause significant changes in the CD spectra, indicating little conformational change on ferrisiderophore binding, which concurs with the findings of X-ray crystallographic studies of other siderophore-binding proteins (*26*).

To verify that the change in tryptophan fluorescence that occurs when ferrioxamine B is added to CdtB results from binding, we used CD spectroscopy to investigate whether the melting temperature of the protein increases in the presence of the ligand. The melting temperature of CdtB alone was 36.4 ± 0.1 °C, whereas the melting temperature of CdtB in the presence of an equimolar concentration of the ligand was 50.2 ± 0.2 °C (see Supporting Information). Thus binding of ferrioxamine B to CdtB significantly stabilizes the protein.

DISCUSSION

The experiments reported here confirm many aspects of the model for cognate siderophore uptake proposed by Barona-Gomez et al. (*10*) on the basis of growth promotion experiments with *S. coelicolor* siderophore nonproducing mutants lacking specific SBPs. In particular, they provide direct evidence for the roles of DesE and CchF as ferrioxamine E and ferricoelichelin receptors, respectively (Figure 7). Ferrioxamine B and the fungal hydroxamate ferrisiderophore ferrichrome are also recognized by DesE. Ferrioxamine B binding by DesE explains the observation that *S. coelicolor* mutants lacking the *cdt* gene cluster are still able to uptake ferrioxamine B (*18*); it is very likely that ferrioxamine B can be taken up by DesE-mediated transport.

DesE was observed to bind ferrialbomycin, which is surprising because *S. coelicolor* is resistant to this antibiotic (*18*). However, the dissociation constant for the DesE−ferrialbomycin complex (0.75 μM) is probably too large to allow efficient ferrialbomycin uptake. Given that DesE binds ferrioxamine E, ferrioxamine B, ferrialbomycin, and ferrichrome, it is tempting to regard it as a general ferric-*tris*-hydroxamate receptor. However, DesE has little affinity for the ferric-*tris*-hydroxamate ferricoelichelin.

The observation that CchF binds only to ferricoelichelin but not other ferrisiderophores of *S. coelicolor* supports the proposal that the *cch* cluster encodes a complete siderophore biosynthetic−export−uptake system (*27*). It is interesting to speculate about the origins of this gene cluster. In addition to *S. coelicolor* and *S. ambofaciens*, it has been found in several other recently sequenced streptomycete genomes, including *Streptomyces griseus* NBRC 13350, *Streptomyces lividans* TK24, *Streptomyces viridochromogenes* DSM 40736, *Streptomyces hygroscopicus* ATCC 53653, and *Streptomyces flavogriseus* ATCC 33331. Unlike the *des* cluster, however, it is not present in all streptomycete genomes sequenced to date. It has been proposed that the production of coelichelin offers a "contingency plan" for iron acquisition in the presence of competitors that can utilize ferrioxamines as iron sources (*27*). Perhaps the *cch* cluster was originally present in all streptomycetes but has been lost by streptomycetes that inhabit environments lacking competitors that can uptake ferrioxamines.

The specificity of CdtB for ferrioxamine B suggests the *cdt* cluster is involved in the uptake of this ferrisiderophore as previously hypothesized (*10*, *18*). Surprisingly, CdtB has about 100 times lower affinity for the structurally very similar ferrioxamine E.

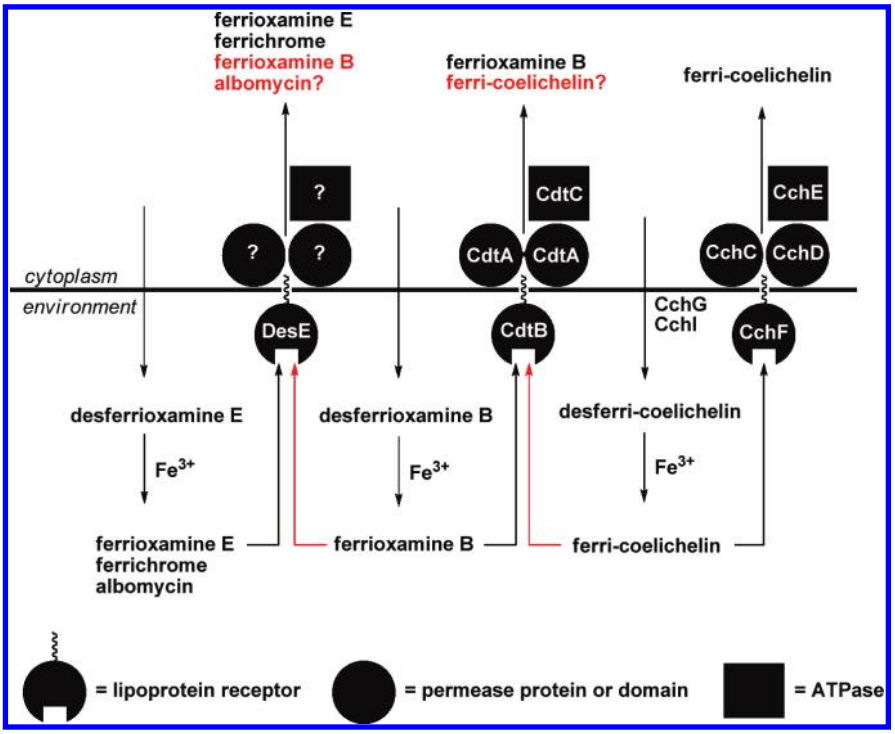

FIGURE 7: Model for ferrisiderophore uptake in *S. coelicolor*. The desferrisiderophores desferrioxamines B and E and desferricoelichelin are excreted by *S. coelicolor*, bind to ferric iron, and are imported into the cell via ABC transporters. The refinements to the previous model (*10*) are highlighted in red. Question marks indicate uncertainty regarding the import of ferrialbomycin and ferricoelichelin by the transporters, despite observed binding to their SBP components (red).

This indicates that there might be different modes of binding of ferrioxamine B to CdtB and DesE. Structural studies should shed light on the molecular basis of the difference in ferrioxamine specificity between DesE and CdtB. The nanomolar dissociation constant of ferricoelichelin−CdtB was surprising, because the *cchCDEF* genes have been shown to be necessary for growth on a colloidal silica medium supplemented with ferricoelichelin (*10*). Thus at least some of these genes are required for efficient ferricoelichelin uptake. It is possible that only the permease and ATPase genes of the *cch* cluster are required and that CdtB can take the role of CchF in ferricoelichelin binding and delivery to the permease. The fate of CdtB−ferricoelichelin could be further investigated by growth promotion experiments with ferricoelichelin using siderophore nonproducing mutants of *S. coelicolor* lacking *cchF* but with the *cdtB* and *cchCDE* genes still present. Such experiments would shed light on whether the permease−ATPase genes in the *cch* cluster can release and transport ferricoelichelin from CdtB. Another possible explanation is that the observed binding of ferricoelichelin to CdtB is not biologically significant. Perhaps the ferricoelichelin−CdtB complex is unable to interact with permeases to allow translocation of the ferrisiderophore. The flexibility of recombinantly purified SBPs is illustrated by the *E. coli* SBP FitE, which crystallized as "open" and "closed" forms (*28*). These two forms were also seen in *E. coli* vitamin B_{12} binding protein BtuF when bound to the permease−ATPase dimer (*3*) in comparison with the "closed" form of apo-BtuF (*29*). If ferrioxamine B and ferricoelichelin bind to CdtB to give open or closed forms, perhaps only one of these forms is recognized by the permease CdtA, with only ferrioxamine B being taken up by the CdtABC system.

In conclusion, we have carried out the first direct biochemical analyses of *Streptomyces* siderophore binding protein substrate specificity. The results of these experiments support previous inferences of substrate specificity derived from genetic experiments and show that *S. coelicolor*, like other Gram-positive bacteria, possesses several extracellular membrane-associated siderophore proteins with high affinity and significantly differing specificity for cognate siderophores. These studies lay the foundations for future research aimed at dissecting the functional significance of multiple distinct systems for siderophore biosynthesis and uptake in *S. coelicolor* and other members of the *Streptomyces* genus.

ACKNOWLEDGMENT

We thank Alison Rodger for helpful discussions and Xujia Hu for assistance with purification of coelichelin.

SUPPORTING INFORMATION AVAILABLE

Chromatograms from gel filtration analyses of purified recombinant DesE, CchF, and CdtB and melting curves for CdtB in the absence/presence of ferrioxamine B. This material is available free of charge via the Internet at http://pubs.acs.org.

REFERENCES

1. Miethke, M., and Marahiel, M. A. (2007) Siderophore-based iron acquisition and pathogen control. *Microbiol. Mol. Biol. Rev. 71*, 413–451.
2. Cendrowski, S., MacArthur, W., and Hanna, P. (2004) *Bacillus anthracis* requires siderophore biosynthesis for growth in macrophages and mouse virulence. *Mol. Microbiol. 51*, 407–417.
3. Hvorup, R. N., Goetz, B. A., Niederer, M., Hollenstein, K., Perozo, E., and Locher, K. P. (2007) Asymmetry in the structure of the ABC transporter-binding protein complex BtuCD-BtuF. *Science 317*, 1387–1390.
4. Zawadzka, A., Abergel, R. J., Nichiporuk, R., Andersen, U. J., and Raymond, K. N. (2009) Siderophore-mediated iron acquisition systems in *Bacillus cereus*: Identification of receptors for anthrax virulence-associated petrobactin. *Biochemistry 48*, 3645–3657.

5. Peuckert, F., Miethke, M., Albrecht, A. G., Essen, L.-O., and Marahiel, M. A. (2009) Structural basis and stereochemistry of triscatecholate siderophore binding by FeuA. *Angew. Chem., Int. Ed. 48*, 7924.
6. Sebulsky, M. T., Shilton, B. H., Speziali, C. D., and Heinrichs, D. E. (2003) The role of FhuD2 in iron(III)-hydroxamate transport in *Staphylococcus aureus*: Demonstration that FhuD2 binds iron(III)-hydroxamates but with minimal conformational change and implication of mutations on transport. *J. Biol. Chem. 278*, 49890–49900.
7. Clancy, A., Loar, J. W., Speziali, C. D., Oberg, M., Heinrichs, D. E., and Rubens, C. E. (2006) Evidence for siderophore-dependent iron acquisition in group B streptococcus. *Mol. Microbiol. 59*, 707–721.
8. Farhana, A., Kumar, S., Rathore, S. S., Ghosh, P. C., Ehtesham, N. Z., Tyagi, A. K., and Hasnain, S. E. (2008) Mechanistic insights into a novel exporter-importer system of *Mycobacterium tuberculosis* unravel its role in trafficking of iron. *PLoS One 3*, e2087.
9. Lautru, S., Deeth, R. J., Bailey, L. M., and Challis, G. L. (2005) Discovery of a new peptide natural product by *Streptomyces coelicolor* genome mining. *Nat. Chem. Biol. 1*, 265–269.
10. Barona-Gomez, F., Lautru, S., Francou, F. X., Leblond, P., Pernodet, J. L., and Challis, G. L. (2006) Multiple biosynthetic and uptake systems mediate siderophore-dependent iron acquisition in *Streptomyces coelicolor* and *Streptomyces ambofaciens*. *Microbiology 152*, 3355–3366.
11. Barona-Gomez, F., Wong, U., Giannakopulos, A. E., Derrick, P. J., and Challis, G. L. (2004) Identification of a cluster of genes that directs desferrioxamine biosynthesis in *Streptomyces coelicolor* M145. *J. Am. Chem. Soc. 126*, 16282–16283.
12. Challis, G. L. (2005) A widely distributed bacterial pathway independent of nonribosomal peptide synthetases for siderophore biosynthesis. *ChemBioChem 4*, 601–611.
13. Kadi, N., Oves-Costales, D., Barona-Gomez, F., and Challis, G. L. (2007) A new family of ATP-dependent oligomerization-macrocyclization biocatalysts. *Nat. Chem. Biol. 3*, 652–656.
14. Tunca, S., Barreiro, C., Sola-Landa, A., Coque, J. J. R., and Martin, J. F. (2007) Transcriptional regulation of the desferrioxamine gene cluster of *Streptomyces coelicolor* is mediated by binding of DmdR1 to an iron box in the promoter of the *desA* gene. *FEBS J. 274*, 1110–1122.
15. Kim, D.-W., Chater, K. F., Lee, K.-J., and Hesketh, A. (2005) Effects of growth phase and the developmentally significant bldA-specified tRNA on the membrane-associated proteome of *Streptomyces coelicolor*. *Microbiology 151*, 2707–2720.
16. Hutchings, M. I., Palmer, T., Harrington, D. J., and Sutcliffe, I. C. (2009) Lipoprotein biogenesis in Gram-positive bacteria: Knowing when to hold em, knowing when to fold em. *Trends Microbiol. 17*, 13–21.
17. Widdick, D. A., Dilks, K., Chandra, G., Bottrill, A., Naldrett, M., Pohlschroder, M., and Palmer, T. (2006) The twin-arginine translocation pathway is a major route of protein export in *Streptomyces coelicolor*. *Proc. Natl. Acad. Sci. U.S.A. 103*, 17927–17932.
18. Bunet, R., Brock, A., Rexer, H.-U., and Takano, E. (2006) Identification of genes involved in siderophore transport in *Streptomyces coelicolor* A3(2). *FEMS Microbiol. Lett. 262*, 57–64.
19. Braun, V., Pramanik, A., Gwinner, T., Köberle, M., and Bohn, E. (2009) Sideromycins: Tools and antibiotics. *Biometals 22*, 3–13.
20. Bradford, M. M. (1976) A rapid and sensitive method for the quantitation of microgram quantities of protein utilizing the principle of protein-dye binding. *Anal. Biochem. 72*, 248–254.
21. Kapust, R. B., Tözsér, J., Fox, J. D., Anderson, D. E., Cherry, S., Copeland, T. D., and Waugh, D. S. (2001) Tobacco etch virus protease: Mechanism of autolysis and rational design of stable mutants with wild-type catalytic proficiency. *Protein Eng. 14*, 993–1000.
22. Origin. 6.0 Professional, Microcal Software Inc.
23. Ahnström, J., Faber, K., Axler, O., and Dahlbäck, B. (2007) Hydrophobic ligand binding properties of the human lipocalin apolipoprotein M. *J. Lipid. Res. 48*, 1754–1762.
24. Matzanke, B. F., Müller-Matzanke, G., and Raymond, K. N. (1989) Iron carriers and iron proteins: Siderophore-mediated iron transport, in Iron Carriers and Iron Proteins (Loehr, T. M., Ed.) VCH Inc., New York.
25. Cantor, C. R., and Schimmel, P. R. (1980) Biophysical Chemistry—Part II: Techniques for the study of biological structure and function, W. H. Freeman, San Francisco.
26. Clarke, T. E., Braun, V., Winkelmann, G., Tari, L. W., and Vogel, H. J. (2002) X-ray crystallographic structures of the *Escherichia coli* periplasmic protein FhuD bound to hydroxamate-type siderophores and the antibiotic albomycin. *J. Biol. Chem. 277*, 13966–13972.
27. Challis, G. L., and Hopwood, D. A. (2003) Synergy and contingency as driving forces for the evolution of multiple secondary metabolite production in *Streptomyces* species. *Proc. Natl. Acad. Sci. U.S.A. 25*, 14555–14561.
28. Shi, R., Proteau, A., Wagner, J., Cui, Q., Purisima, E. O., Matte, A., and Cygler, M. (2009) Trapping open and closed forms of FitE-A group III periplasmic binding protein. *Proteins 75*, 598–605.
29. Karpowich, N. K., Huang, H. H., Smith, P. C., and Hunt, J. F. (2003) Crystal structures of the BtuF periplasmic-binding protein for vitamin B12 suggest a functionally important reduction in protein mobility upon ligand binding. *J. Biol. Chem. 278*, 8429–8434.